Atomistic Simulation and the Mechanism of Graphene Amorphization under Electron Irradiation

Supplementary Information

Zilin Liang,[a] Ziwei Xu,[b] Tianying Yan,[*a] and Feng Ding[*b]

[a] *Tianjin Key Laboratory of Metal- and Molecule-Based Material Chemistry, Synergetic Innovation Center of Chemical Science and Engineering (Tianjin), Key Laboratory of Advanced Energy Materials Chemistry (Ministry of Education), Institute of New Energy Material Chemistry, College of Chemistry, Nankai University, Tianjin 300071, China. Email: tyan@nankai.edu.cn*
[b] *Institute of Textiles and Clothing, Hong Kong Polytechnic University, Hung Hom, Hong Kong, China. Email: tcfding@inet.polyu.edu.hk*

Computational Methods

We used nonequlibrium molecular dynamic (NEMD) simulation to study the reconstruction from divacancy (V_2) to the amorphous structure on a suspended single-layer graphene under electron irradiation (EI). Interaction of carbon atoms is simulated with the second generation of Brenner, namely, the REBO2 potential,[1] which has been successfully applied in previous simulation of EI and ion bombardment on carbon nanotube and graphene.[2-6] The EI process is simulated with the elastic collision model between a randomly selected carbon atom in the irradiation area and an incident electron perpendicular to the suspended graphene layer. The transferred energy (E_t) and the scattering polar angle θ of the target carbon upon collision are given by,[4, 6]

$$E_t = [1 - (\frac{m_e \cos\theta + \sqrt{m_c^2 - m_e^2 \sin^2\theta}}{m_e + m_c})^2] E_i \quad \text{(S1)}$$

$$\cos\theta = \sqrt{\frac{(m_e + m_c)^2 E_t}{4 m_e m_c E_0}} \quad \text{(S2)}$$

in which m_c and m_e are the mass of carbon atom and electron, E_0 is the energy of incident electron. The azimuzal angel φ of the scattered carbon atom is sampled uniformly from 0° to 360°. In Eq. (S1), the scattering angel ω of the incident electron is sampled from a screened Rutherford cross section.

The graphene lattice with a $V_2(5|8|5)$ in the center is composed of 798 carbon atoms with two-dimensional periodic boundary condition applied on x-y plane. The radius of irradiation area is 15 Å around the center of the graphene, while the carbon atoms beyond 20 Å to the center of the graphene are coupled to Nosé-Hoover-chain thermostat[7, 8] of 2000K. The center of the suspended graphene layer is constrained on the origin by removing the parallel component of the center-of-mass velocity of the suspended graphene along the EI direction at each MD integration step, so that there is no overall translational motion of the suspended graphene even exposed to continuous EI. The simulation model is depicted in Fig. S1.

Ten independent MD simulations were carried out for 100 ns with a time step of 0.5 fs, and each trajectory was run for 100 ns for 80 keV and 60 keV EI. Due to the incomparable time scale of MD simulation and experiment, the intensity of electron beam is set to be $8.9\text{x}10^{14}$ e·nm^2 s^{-1} ($1.4\text{x}10^{10}$ A • cm^{-2}), which is 5-8 order of magnitude higher than a typical experimental EI intensity, but the electron dose is comparable with the experimental measurements.[9-11] The graphene lattice, with a ground structure $V_2(5|8|5)$ in its center, is bombarded by the incident electrons of 80 keV and 60 keV, respectively, for

observing the evolution from point defect toward various amorphous structures. Using Eq. (S1), the maximum E_t of the incident electron of 80 and 60 keV are 14.7 eV and 11.0 eV respectively, which is high enough to stimulate a generalized Stone-Wales transformation (GSWT), but not energetic to knock out a carbon atom.[12]

In order to well understand the mechanism of the reconstruction and compare with NEMD simulation in a consistent manner, the formation energy (E_f) as well as the GSWT barrier (ΔE) are also calculated with REBO2 potential, i.e.,

$$E_f = E(N-n) + n\mu_C - E(N) \qquad \text{(S3)}$$

in which *E(N-n)* is the system energy with *n* atom missing, μ_C is the chemical potential for each carbon and *E(N)* is the system energy of the pristine graphene. ΔE's of GSWTs are calculated by the climbing image nudged elastic band (CI-NEB) method.[13, 14] E_f's and ΔE's of the GSWTs, calculated by the REBO2 potential, is in reasonable agreement with the known DFT results, as shown in Fig. 1 of the main text. Specifically, the E_f, ΔE, and backward barrier (ΔE_r) of Stone-Wales transformation on the pristine graphene, optimized by REBO2 potential, are 5.2 eV, 8.8 eV, and 3.6 eV, which are in reasonable agreement with the DFT result of, 4.8-5.3 eV, 9.2 eV, and 4.4 eV, respectively.[15, 16] The NEMD simulations and the geometric optimizations (E_f's and ΔE's) were performed by a home-made code.

References

1. D. W. Brenner, O. A. Shenderova, J. A. Harrison, S. J. Stuart, B. Ni and S. B. Sinnott, *J. Phys.: Condens. Matter*, 2002, **14**, 783-802.
2. A. V. Krasheninnikov, K. Nordlund and J. Keinonen, *Phys. Rev. B*, 2002, **65**, 165423.
3. I. Jang, S. B. Sinnott, D. Danailov and P. Keblinski, *Nano Lett.*, 2003, **4**, 109-114.
4. M. Yasuda, Y. Kimoto, K. Tada, H. Mori, S. Akita, Y. Nakayama and Y. Hirai, *Phys. Rev. B*, 2007, **75**, 205406.
5. O. Lehtinen, J. Kotakoski, A. V. Krasheninnikov, A. Tolvanen, K. Nordlund and J. Keinonen, *Phys. Rev. B*, 2010, **81**, 153401.
6. M. Yasuda, R. Mimura, H. Kawata and Y. Hirai, *J. Appl. Phys.*, 2011, **109**, 054304-054305.
7. G. J. Martyna, M. E. Tuckerman, D. J. Tobias and M. L. Klein, *Mol. Phys.*, 1996, **87**, 1117-1157.
8. M. E. Tuckerman, Y. Liu, G. Ciccotti and G. J. Martyna, *J. Chem. Phys.*, 2001, **115**, 1678-1702.
9. J. Kotakoski, A. V. Krasheninnikov, U. Kaiser and J. C. Meyer, *Phys. Rev. Lett.*, 2011, **106**, 105505.
10. A. W. Robertson, C. S. Allen, Y. A. Wu, K. He, J. Olivier, J. Neethling, A. I. Kirkland and J. H. Warner, *Nat. Commun.*, 2012, **3**, 1144.
11. J. C. Meyer, F. Eder, S. Kurasch, V. Skakalova, J. Kotakoski, H. J. Park, S. Roth, A.

Chuvilin, S. Eyhusen, G. Benner, A. V. Krasheninnikov and U. Kaiser, *Phys. Rev. Lett.*, 2012, **108**, 196102.

12. J. Kotakoski, J. C. Meyer, S. Kurasch, D. Santos-Cottin, U. Kaiser and A. V. Krasheninnikov, *Phys. Rev. B*, 2011, **83**, 245420.

13. G. Henkelman and H. Jonsson, *J. Chem. Phys.*, 2000, **113**, 9978-9985.

14. G. Henkelman, B. P. Uberuaga and H. Jonsson, *J. Chem. Phys.*, 2000, **113**, 9901-9904.

15. L. Li, S. Reich and J. Robertson, *Phys. Rev. B*, 2005, **72**, 184109.

16. J. Ma, D. Alfé, A. Michaelides and E. Wang, *Phys. Rev. B*, 2009, **80**, 033407.

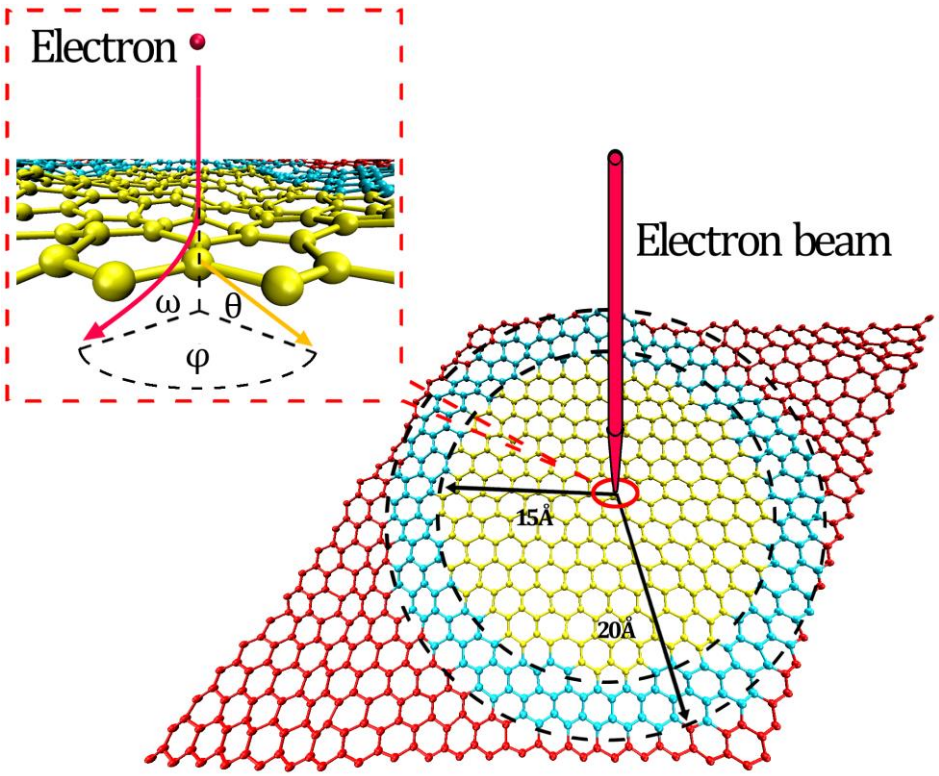

Fig. S1. Illustration of the EI model in the NEMD simulations. The irradiation area and the area coupled to a thermostat are marked as yellow and red, respectively, while the area in between marked as blue. The scattering angle of electron, ω, the scattering polar angel of carbon, θ, and the azimuzal angel of carbon, φ, are depicted in the upper-left inset.